

Entropy-based random models for hypergraphs

Fabio Saracco,^{1,2,3} Giovanni Petri,⁴ Renaud Lambiotte,⁵ and Tiziano Squartini^{3,6}

¹*‘Enrico Fermi’ Research Center (CREF), Via Panisperna 89A, 00184 Rome (Italy)*

²*Institute for Applied Computing ‘Mauro Picone’ (IAC),*

National Research Council, Via dei Taurini 19, 00185 Rome (Italy)

³*IMT School for Advanced Studies, Piazza San Francesco 19, 55100 Lucca (Italy)**

⁴*CENTAI, Corso Inghilterra 3, 10136 Turin (Italy)*

⁵*Mathematical Institute, University of Oxford, Woodstock Road, OX2 6GG Oxford (United Kingdom)*

⁶*Institute for Advanced Study (IAS), University of Amsterdam,
Oude Turfmarkt 145, 1012 GC Amsterdam (The Netherlands)*

(Dated: July 26, 2022)

Network science has traditionally focused on pairwise relationships while disregarding many-body interactions. Hypergraphs are promising mathematical objects for the description of the latter ones. Here, we propose null models to analyse hypergraphs that generalise the classical Erdős-Rényi and Configuration Model by randomising incidence matrices in a constrained fashion. After discussing them, we extend the definition of several network quantities to hypergraphs, derive their expected values and compare them with empirical ones, to detect significant deviations from random behaviours.

PACS numbers: 89.75.Fb; 02.50.Tt

Introduction. Networks provide a powerful language to model interacting systems [1, 2]. Within a network framework, the basic unit of interaction, i.e. the edge, involves two nodes and the complexity of the structure as a whole arises from the complex combination of these units. Despite its many successes, network science disregards certain aspects of interacting systems, notably the possibility that more-than-two constituent units could interact at a time [3]. Yet, it has been increasingly shown that, for a variety of systems, interactions cannot be always decomposed in a pairwise fashion and that neglecting higher-order ones can lead to incomplete, if not misleading, representations [3]. Examples include chemical-reactions involving several compounds, coordination activities within small teams of people working together, brain activities mediated by groups of neurons [4]. Generally speaking, thus, modelling the joint coordination of multiple entities calls for a framework that generalises the traditional, edge-centered one. An increasingly popular alternative to support ‘a science’ of many-body interactions is provided by hypergraphs as these versatile mathematical objects naturally allow nodes to interact ‘in groups’ [5].

Given the recent interest towards such objects, the definition of analytical tools to study them is still in its infancy [6–8]. The present paper represents our contribution to fill this gap: hereby, we extend the class of entropy-based null models [9, 10] to hypergraphs. These models work by preserving a given set of quantities while randomising everything else, hence destroying all possible correlations between structural properties except for the ones genuinely encoded in the constraints themselves [11–13]. The versatility of such an approach allows it to be employed either in presence of full information - to spot the degree of self-organisation of a network

by detecting the patterns that are not explained by lower-level constraints [14–18] - or in presence of partial information - to infer the missing portion(s) of a given network [19].

Our strategy to define null models for hypergraphs is based on the randomisation of their incidence matrix, i.e. the (generally, rectangular) matrix containing information about the connectivity of nodes, i.e. the set of hyperedges they belong to, and the connectivity of hyperedges, i.e. the set of nodes they ‘cluster’.

Formalism and basic quantities. A hypergraph can be defined as a pair $H(\mathcal{V}, \mathcal{E}_H)$ where \mathcal{V} is the set of vertices and \mathcal{E}_H is the set of hyperedges. While for a traditional graph $G(\mathcal{V}, \mathcal{E}_G)$, the edge set \mathcal{E}_G is a subset of the cartesian product $\mathcal{V} \times \mathcal{V}$, for an hypergraph $H(\mathcal{V}, \mathcal{E}_H)$, the hyperedge set \mathcal{E}_H is a subset of the power set of \mathcal{V} : the presence of subsets of nodes with cardinality different from two is, thus, allowed.

As for traditional graphs, an algebraic representation of hypergraphs can be devised as well. Let us call the cardinality of the set of nodes $|\mathcal{V}| = N$ and the cardinality of the set of hyperedges $|\mathcal{E}_H| = L$ (for a formal analogy with the traditional case): then, we consider the $N \times L$ table known as incidence matrix, each row of which corresponds to a node and each column of which corresponds to an hyperedge. If we indicate the incidence matrix with \mathbf{I} , its generic entry $I_{i\alpha}$ will be 1 if vertex i belongs to hyperedge α and 0 otherwise. Notice that the number of 1s along each row can vary between 0 and L , the former case indicating a disconnected node and the latter one indicating a node that belongs to each hyperedge; similarly, the number of 1s along each columns can vary between 1 and N , the former case indicating that the hyperedge includes only one node and the latter one indicating that the hyperedge includes all

$$\mathbf{I} = \begin{array}{c|ccccc} & \mathbf{e}_1 & \mathbf{e}_2 & \mathbf{e}_3 & \mathbf{e}_4 & \mathbf{e}_5 \\ \hline \mathbf{n}_1 & 0 & 1 & 1 & 0 & 1 \\ \mathbf{n}_2 & 0 & 0 & 1 & 1 & 1 \\ \mathbf{n}_3 & 0 & 1 & 1 & 1 & 0 \\ \mathbf{n}_4 & 1 & 0 & 0 & 1 & 1 \\ \mathbf{n}_5 & 1 & 1 & 1 & 1 & 0 \\ \mathbf{n}_6 & 0 & 1 & 0 & 0 & 0 \end{array}$$

TABLE I: Example of incidence matrix describing a binary, undirected hypergraph with 6 nodes and 5 hyperedges. The generic entry $I_{i\alpha}$ is 1 if vertex i belongs to hyperedge α and 0 otherwise (see also Fig. 1).

nodes. Table I represents the incidence matrix describing the binary, undirected hypergraph shown in Fig. 1.

Once the incidence matrix has been defined, several quantities needed for the description of hypergraphs can be defined quite straightforwardly: for example, the ‘degree’ of node i reads $k_i = \sum_{\alpha=1}^L I_{i\alpha}$ and counts the number of hyperedges that are incident to it; analogously, the ‘degree’ of the hyperedge α (i.e. its hyperdegree) reads $h_\alpha = \sum_{i=1}^N I_{i\alpha}$ and counts the number of nodes it ‘includes’; both the sum of degrees and that of hyperdegrees equal the total number of 1s, i.e. $\sum_{i=1}^N k_i = \sum_{i=1}^N \sum_{\alpha=1}^L I_{i\alpha} = \sum_{\alpha=1}^L h_\alpha \equiv T$. Importantly, the degree of a node no longer coincides with the number of its neighbours: instead, it matches the number of hyperedges it belongs to; the hyperdegree, instead, provides information on the hyperedge size.

Randomisation of binary hypergraphs. Early attempts to define randomisation models for hypergraphs can be found in [20]: there, however, the authors have just considered hyperedges that are incident to triples of nodes; the same framework has been applied to study the World Trade Network [7]. Considering the incidence matrix has, however, two clear advantages: (i) *generality*, because the incidence matrix allows hyperedges of any size to be handled at once; (ii) *compactness*, because the order of tensor \mathbf{I} never exceeds two and allows any hypergraph to be represented as a traditional, bipartite graph - the two layers of the latter being now defined by nodes and hyperedges [7].

In order to extend the rich set of null models defined by graph-specific global and local constraints to hypergraphs, we first need to identify the quantities that can play those roles. In what follows, we will consider the total number of 1s, i.e. T , the degree and the hyperdegree sequences, i.e. $\{k_i\}_{i=1}^N$ and $\{h_\alpha\}_{\alpha=1}^L$ - either separately or in a joint fashion; moreover, we will distinguish between microcanonical and canonical randomisation techniques.

Random Hypergraph Model (RHM). The model is defined by just one global constraint that, in our case, reads $T = \sum_{i=1}^N \sum_{\alpha=1}^L I_{i\alpha}$. Its microcanonical version extends the model by Erdős and Rényi [21] - also known

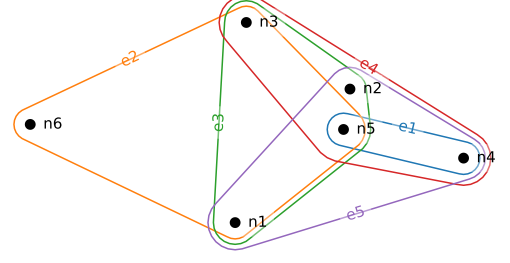


FIG. 1: Cartoon representation of the hypergraph whose incidence matrix is shown in Table I.

as Random Graph Model (RGM) - to hypergraphs and prescribes to count the number of incidence matrices that are compatible with a given, total number of 1s, say T^* : they are

$$\Omega_{\text{RHM}} = \binom{V}{T^*} \quad (1)$$

with $V = NL$ being the total number of entries of the incidence matrix \mathbf{I} . Once the total number of configurations composing the microcanonical ensemble is determined, a procedure to generate them is needed: in the case of the RHM, it simply boils down to reshuffling the entries of the incidence matrix, a procedure ensuring that the total number of 1s is kept fixed while any other correlation is destroyed.

The canonical version of the RHM, instead, extends the model by Gilbert [22] and rests upon the constrained maximisation of Shannon entropy, i.e.

$$\mathcal{L} = S[P] - \sum_{i=0}^M \theta_i [P(\mathbf{I}) C_i(\mathbf{I}) - \langle C_i \rangle] \quad (2)$$

where $S[P] = -\sum_{\mathbf{I}} P(\mathbf{I}) \ln P(\mathbf{I})$, $C_0 \equiv \langle C_0 \rangle \equiv 1$ sums up the normalization condition and the remaining $M - 1$ constraints represent proper, topological properties. Such an optimisation procedure defines the *Exponential Random Hypergraph* (ERH) framework, described by the expression

$$P(\mathbf{I}) = \frac{e^{-H(\mathbf{I})}}{Z} = \frac{e^{-H(\mathbf{I})}}{\sum_{\mathbf{I}} e^{-H(\mathbf{I})}}. \quad (3)$$

In the simplest case, there is just one global constraint represented by T , leading to the expression

$$\begin{aligned} P(\mathbf{I}) &= \frac{e^{-\theta T}}{\sum_{\mathbf{I}} e^{-\theta T}} = \frac{e^{-\sum_{i,\alpha} \theta I_{i\alpha}}}{\sum_{\mathbf{I}} e^{-\sum_{i,\alpha} \theta I_{i\alpha}}} = \prod_{i=1}^N \prod_{\alpha=1}^L \frac{x^{I_{i\alpha}}}{1+x} \\ &= p^T (1-p)^{NL-T} \end{aligned} \quad (4)$$

where $e^{-\theta} \equiv x$ and $p \equiv x/(1+x)$. The canonical ensemble, now, includes all $N \times L$ rectangular matrices whose number of entries equating 1 ranges from 0 to NL . According to such a model, the entries of the incidence matrix are i.i.d. Bernoulli random variables, i.e. $I_{i\alpha} \sim \text{Ber}(p)$, $\forall i, \alpha$: as a consequence, the total number of 1s, the degrees and the hyperdegrees obey binomial distributions - being all defined as sums of i.i.d. Bernoulli random variables. Specifically, $T \sim \text{Bin}(NL, p)$, $k_i \sim \text{Bin}(L, p)$, $\forall i$ and $h_\alpha \sim \text{Bin}(N, p)$, $\forall \alpha$, in turn, implying that $\langle T \rangle_{\text{RHM}} = NLp$, $\langle k_i \rangle_{\text{RHM}} = Lp$, $\forall i$ and $\langle h_\alpha \rangle_{\text{RHM}} = Np$, $\forall \alpha$.

In order to ensure that $\langle T \rangle_{\text{RHM}} = T^*$, parameters have to be tuned opportunely. To this aim, the likelihood maximisation principle can be invoked [23]: it prescribes to maximise the function $\mathcal{L}(\theta) \equiv \ln P(\mathbf{I}|\theta)$ with respect to the unknown parameter(s) that define it. Such a recipe leads us to find $p = T^*/(NL)$.

Hypergraph Configuration Model (HCM). The number of constraints can be enlarged to include the degrees, i.e. the sequence $\{k_i\}_{i=1}^N$, and the hyperdegrees, i.e. the sequence $\{h_\alpha\}_{\alpha=1}^L$. Counting the number of configurations on which both degree sequences match their empirical values is a hard task - although numerical recipes to shuffle the entries of a rectangular matrix, while preserving its marginals, exist [6, 24, 25]; solving the corresponding problem in the canonical framework is, instead, straightforward. Indeed, Shannon entropy maximisation leads to

$$\begin{aligned} P(\mathbf{I}) &= \frac{e^{-\sum_i \alpha_i k_i - \sum_\alpha \beta_\alpha h_\alpha}}{\sum_{\mathbf{I}} e^{-\sum_i \alpha_i k_i - \sum_\alpha \beta_\alpha h_\alpha}} = \frac{e^{-\sum_{i,\alpha} (\alpha_i + \beta_\alpha) I_{i\alpha}}}{\sum_{\mathbf{I}} e^{-\sum_{i,\alpha} (\alpha_i + \beta_\alpha) I_{i\alpha}}} \\ &= \prod_{i=1}^N x_i^{k_i} \prod_{\alpha=1}^L y_\alpha^{h_\alpha} \prod_{i=1}^N \prod_{\alpha=1}^L (1 + x_i y_\alpha)^{-1} \\ &= \prod_{i=1}^N \prod_{\alpha=1}^L p_{i\alpha}^{I_{i\alpha}} (1 - p_{i\alpha})^{1-I_{i\alpha}} \end{aligned} \quad (5)$$

where $e^{-\alpha_i} \equiv x_i$, $\forall i$, $e^{-\beta_\alpha} \equiv y_\alpha$, $\forall \alpha$ and $p_{i\alpha} \equiv x_i y_\alpha / (1 + x_i y_\alpha)$, $\forall i, \alpha$. According to such a model, the entries of the incidence matrix of an hypergraph are independent random variables that obey different Bernoulli probability mass functions, i.e. $I_{i\alpha} \sim \text{Ber}(p_{i\alpha})$, $\forall i, \alpha$. As a consequence, both degrees and hyperdegrees obey Poisson-Binomial distributions [15]. In this case, solving the likelihood maximisation problem amounts at solving the system of coupled equations

$$k_i^* = \sum_{\alpha=1}^L \frac{x_i y_\alpha}{1 + x_i y_\alpha} = \sum_{\alpha=1}^L p_{i\alpha} = \langle k_i \rangle, \quad \forall i \quad (6)$$

$$h_\alpha^* = \sum_{i=1}^N \frac{x_i y_\alpha}{1 + x_i y_\alpha} = \sum_{i=1}^N p_{i\alpha} = \langle h_\alpha \rangle, \quad \forall \alpha \quad (7)$$

ensuring that $\langle k_i \rangle = k_i^*$, $\forall i$, $\langle h_\alpha \rangle = h_\alpha^*$, $\forall \alpha$ (and, as a consequence, $\langle T \rangle = T^*$). In case hypergraphs are sparse and in absence of hubs, $p_{i\alpha} \simeq x_i y_\alpha = k_i^* h_\alpha^* / T^*$, $\forall i, \alpha$ (see Appendix A). The HCM reduces to a ‘partial’ Configuration Model [15] when one of two degree sequences is left unconstrained (see Appendix B).

Remarkably, the canonical ensemble of each randomisation model (Table II in Appendix B sums up the set of constraints defining them) can be explicitly sampled by considering each entry of \mathbf{I} , drawing a real number $u_{i\alpha} \in U[0, 1]$ and posing $I_{i\alpha} = 1$ if $u_{i\alpha} \leq p_{i\alpha}$, $\forall i, \alpha$.

Results. The canonical formalism described above leads to factorisable distributions, i.e. distributions that can be written as a product of pair-wise probability mass functions; this allows the expectation of several quantities of interest to be evaluated analytically. To this aim, let us consider the matrix introduced in [4], reading

$$\mathbf{W} = \mathbf{I} \cdot \mathbf{I}^T - \mathbf{K} \quad (8)$$

where \mathbf{K} is the diagonal matrix whose i -th entry reads k_i ; according to the definition above

$$w_{ij} = \sum_{\alpha=1}^L I_{i\alpha} I_{j\alpha} - \delta_{ij} k_i \quad (9)$$

counts the number of hyperedges nodes i and j are connected by - in fact, $w_{ij} = \sum_{\alpha=1}^L I_{i\alpha} I_{j\alpha}$, $i \neq j$ and $w_{ii} = \sum_{\alpha=1}^L I_{i\alpha} I_{i\alpha} - k_i = \sum_{\alpha=1}^L I_{i\alpha} - k_i = k_i - k_i = 0$. The null models discussed so far can be used to estimate $\langle w_{ij} \rangle$ that, in a perfectly general fashion, reads

$$\langle w_{ij} \rangle = \sum_{\alpha=1}^L \langle I_{i\alpha} I_{j\alpha} \rangle = \sum_{\alpha=1}^L \langle I_{i\alpha} \rangle \langle I_{j\alpha} \rangle = \sum_{\alpha=1}^L p_{i\alpha} p_{j\alpha}. \quad (10)$$

The total number of hyperedges shared by node i with any other node in the hypergraph (in a sense, its ‘strength’) can also be computed as

$$\sigma_i = \sum_{j(\neq i)=1}^N w_{ij} = \sum_{j(\neq i)=1}^N \sum_{\alpha=1}^L I_{i\alpha} I_{j\alpha} \quad (11)$$

whose expected value is

$$\langle \sigma_i \rangle = \sum_{j(\neq i)=1}^N \langle w_{ij} \rangle = \sum_{\alpha=1}^L p_{i\alpha} (\langle h_\alpha \rangle - p_{i\alpha}). \quad (12)$$

Assortativity. The quantity above allows us to extend quite naturally the concept of assortativity to hypergraphs, by posing $k_i^{nn} = \sigma_i / k_i = \sum_{\alpha=1}^L I_{i\alpha} h_\alpha / k_i$,

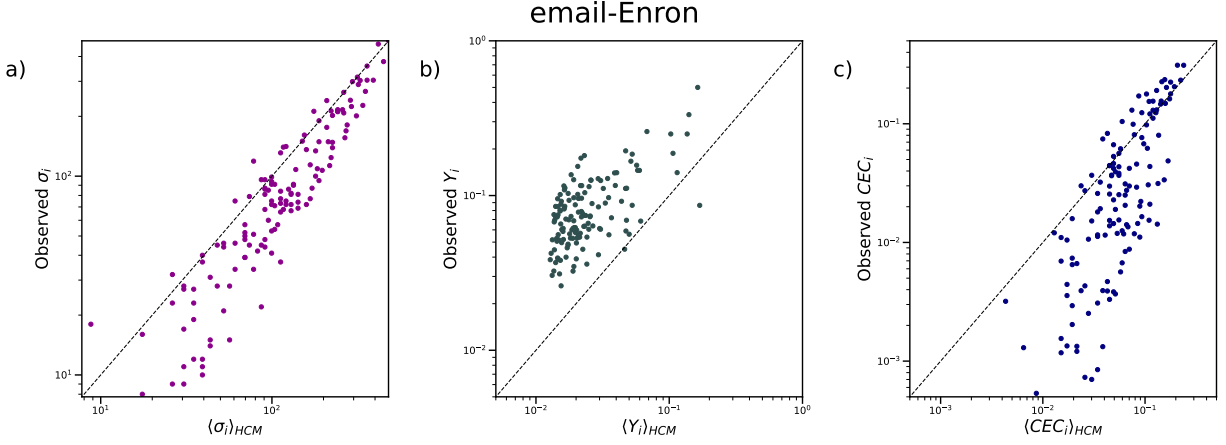


FIG. 2: Scatter plots between the empirical values $\{\sigma_i\}$, $\{Y_i\}$, $\{CEC_i\}$ and the expected values $\{(\sigma_i)_{HCM}\}$, $\{(Y_i)_{HCM}\}$, $\{(CEC_i)_{HCM}\}$. The HCM overestimates the extent to which any two nodes overlap, as well as the CEC; the disparity ratio, instead, is underestimated by it. These results can be understood by considering that the HCM just constrains the degree sequences, hence ‘distributing’ connections more homogeneously than observed.

a quantity that represents the arithmetic mean of the degrees of the hyperedges including node i . An analytical approximation of its expected value can be provided as well and reads $\langle k_i^{nn} \rangle \simeq \langle \sigma_i \rangle / \langle k_i \rangle$, $\forall i$ (Fig. 2a).

Disparity ratio. More information about the patterns shaping real-world hypergraphs can be obtained upon defining the ratios $f_{ij} = w_{ij}/\sigma_i$, $\forall i \neq j$ inducing the quantity

$$Y_i = \sum_{j(\neq i)=1}^N f_{ij}^2 = \sum_{j(\neq i)=1}^N \left(\frac{w_{ij}}{\sigma_i} \right)^2 \quad (13)$$

known as disparity ratio and quantifying the (un)evenness of the distribution of the weights constituting the strength of node i over the $\kappa_i = \sum_{j=1}^N \Theta[w_{ij}]$ links characterising its connectivity - where $\Theta[w_{ij}] = 1$ if nodes i and node j share, at least, one hyperedge. More precisely, $Y_i = 1/\kappa_i$ in case weights are equally distributed among the connections established by node i , i.e. $w_{ij} = a_{ij}\sigma_i/\kappa_i$, $\forall j$, any larger value signalling an excess concentration of weight in one or more links. An analytical approximation of its expected value can be provided as well and reads $\langle Y_i \rangle \simeq \sum_{j(\neq i)=1}^N \langle w_{ij}^2 \rangle / \langle \sigma_i^2 \rangle$, $\forall i$ (see Fig. 2b for comparison) - but there are caveats (see Appendix C for details).

Eigenvector centrality. Centrality measures for hypergraphs have been defined as well. An example is provided by the clique motif eigenvector centrality (CEC) defined in [26]: CEC_i corresponds to the i -th entry of the Perron-Frobenius eigenvector of \mathbf{W} (Fig. 2c).

Confusion matrix. So far, we have dealt with global quantities. Let us now consider the set of local properties composing the so-called confusion matrix. They are

known as the true positive rate (TPR) defined as the percentage of 1s correctly recovered by a given method and whose expected value reads $\langle TPR \rangle = \sum_{i<j} I_{i\alpha} p_{i\alpha} / T$, the specificity (SPC) defined as the percentage of 0s correctly recovered by a given method and whose expected value reads $\langle SPC \rangle = \sum_{i<j} (1 - I_{i\alpha})(1 - p_{i\alpha}) / (NL - T)$, the positive predictive value (PPV) defined as the percentage of 1s correctly recovered by a given method with respect to the total number of 1s predicted by it and whose expected value reads $\langle PPV \rangle = \sum_{i<j} I_{i\alpha} p_{i\alpha} / \langle T \rangle$ and the accuracy (ACC), measuring the overall performance of a given method in correctly placing both 1s and 0s and whose expected value reads $\langle ACC \rangle = (\langle TP \rangle + \langle TN \rangle) / NL$ (see Appendix D).

Results on the confusion matrix of a number of real-world hypergraphs reveal that the large sparsity of the latter ones makes it difficult to reproduce the TPR and the PPV (see Table III in Appendix D); on the other hand, the capability of the HCM (both in its ‘full’ and approximated version) to reproduce the density of 1s - and, as a consequence, the density of 0s - ensures the SPC to be recovered quite precisely, in turn ensuring the overall accuracy of the model to be large.

Discussion. First, let us comment on the goodness of the approximation $p_{i\alpha} \simeq x_i y_\alpha = k_i^* h_\alpha^* / T^*$, $\forall i, \alpha$. Overall, it is quite accurate for the three data sets considered here, i.e. one can safely assume that $x_i \simeq k_i^* / \sqrt{T^*}$, $\forall i$ and $h_\alpha^* / \sqrt{T^*}$, $\forall \alpha$ - and, as a consequence, that $\langle \sigma_i \rangle_{HCM} \simeq k_i^* \sum_{\alpha=1}^L (h_\alpha^*)^2 / T^*$, $\forall i$ (see Fig. 3 in Appendix A).

On the other hand, the expected value of the disparity ratio cannot always be safely decomposed as the ratio of expected values - not even if the ‘full’ HCM is employed. In fact, while this approximation works relatively well

for the `contact-primary-school` data set, it does not for the `email-Enron` and the `NDC-classes` ones (see Fig. 4 in Appendix C). For this reason, to evaluate the expected value of the disparity ratio, we explicitly sampled the ensemble of incidence matrices induced by the ‘full’ HCM.

In general, how accurately the models above reproduce patterns of real-world hypergraphs strongly depends on the system under analysis. Figure 2 shows the results for the `email-Enron` data set: on the one hand, the HCM overestimates the extent to which any two nodes overlap - i.e. real-world hypergraphs are more compartmentalised than expected - and, in turn, overestimates the CEC as well; on the other one, it underestimates the disparity ratio instead. These results can be understood by considering that the HCM constrains only the degree sequences; this leads connections to be distributed more homogeneously than observed, letting the nodes overlap more, thus causing the corresponding entries of \mathbf{W} to be larger (as well as its Perron-Frobenius eigenvector) and more similar. Ultimately, this levels out the differences between the concentrations of weight on different connections.

For the same reason, in presence of largely sparse matrices (and in absence of other constraints), the HCM is prone to yield a large number of false positives while keeping the number of false negatives low (for an overall evaluation of the HCM performance in reproducing real-world hypergraphs, see Table IV in Appendix F).

Conclusions. Our paper contributes to current research on hypergraphs by extending the constrained entropy-maximisation framework to incidence matrices, i.e. their simplest tabular representation. Differently from currently-available techniques [6], our method has the advantage of being analytically tractable and versatile enough as to be easily extensible to directed and/or weighted hypergraphs. Beside their theoretical relevance, our results are particularly useful for detecting patterns that are not imputable to purely random effects. Real-world hypergraphs are, in fact, characterized by a degree of self-organization that is absolutely non-trivial: for instance, the HCM overestimates the extent to which any two nodes overlap, a result whose relevance becomes evident as soon as one considers the different effects higher-order structures have on spreading and cooperation processes [27–29].

Acknowledgements. RL acknowledges support from the EPSRC grants n. EP/V013068/1 and EP/V03474X/1. TS acknowledges support from the EU H2020 project ‘SoBigData++’, grant n. 871042.

* fabio.saracco@cref.it

- [1] M. Newman, *Networks: an introduction* (Oxford University Press, New York, USA, 2010).
- [2] G. Caldarelli, *Scale-free networks* (Oxford University Press, Oxford, UK, 2010).
- [3] R. Lambiotte, M. Rosvall, and I. Scholtes, *Nature Physics* **15**, 313 (2019).
- [4] F. Battiston, G. Cencetti, I. Iacopini, V. Latora, M. Lucas, A. Patania, J. G. Young, and G. Petri, *Physics Reports* **874**, 1 (2020).
- [5] F. Battiston, E. Amico, A. Barrat, G. Bianconi, G. F. de Arruda, B. Franceschiello, I. Iacopini, S. Kéfi, V. Latora, Y. Moreno, M. M. Murray, T. P. Peixoto, F. Vaccarino, and G. Petri, *Nature Physics* **17**, 1093–1098 (2021).
- [6] P. S. Chodrow, *Journal of Complex Networks* **8**, 3 (2020).
- [7] K. Nakajima, K. Shudo, and N. Masuda, *arXiv preprint arXiv:2106.12162* (2021).
- [8] F. Musciotto, F. Battiston, and R. N. Mantegna, *Communications Physics* **4**, 218 (2021).
- [9] E. Jaynes, *The Physical Review* **106**, 181 (1957).
- [10] J. Park and M. E. J. Newman, *Physical Review E* **70**, 66117 (2004).
- [11] T. Squartini and D. Garlaschelli, *New Journal of Physics* **13**, 083001 (2011).
- [12] G. Cimini, T. Squartini, F. Saracco, D. Garlaschelli, A. Gabrielli, and G. Caldarelli, *Nature Reviews Physics* **1**, 58 (2018).
- [13] T. Squartini, G. Caldarelli, G. Cimini, A. Gabrielli, and D. Garlaschelli, *Physics Reports* **757**, 1 (2018).
- [14] T. Squartini, I. van Lelyveld, and D. Garlaschelli, *Scientific Reports* **3**, 3357 (2013).
- [15] F. Saracco, M. J. Straka, R. Di Clemente, A. Gabrielli, G. Caldarelli, and T. Squartini, *New Journal of Physics* **19**, 16 (2017).
- [16] C. Becatti, G. Caldarelli, R. Lambiotte, and F. Saracco, *Palgrave Communications* **5**, 1 (2019).
- [17] G. Caldarelli, R. D. Nicola, F. D. Vigna, M. Petrocchi, F. Saracco, F. D. Vigna, M. Petrocchi, and F. Saracco, *Communications Physics* **3**, 1 (2020).
- [18] Z. P. Neal, R. Domagalski, and B. Sagan, *Scientific Reports* **11**, 23929 (2021).
- [19] F. Parisi, T. Squartini, and D. Garlaschelli, *New Journal of Physics* **22**, 053053 (2020).
- [20] G. Ghoshal, V. Zlatic, G. Caldarelli, and M. E. J. Newman, *Physical Review E* **79**, 066118 (2009).
- [21] P. Erdős and A. Rényi, *Publicationes Mathematicae* **6**, 290 (1959).
- [22] E. N. Gilbert, *The Annals of Mathematical Statistics* **30**, 1141 (1959).
- [23] D. Garlaschelli and M. I. Loffredo, *Physical Review E* **78**, 1 (2008).
- [24] G. Strona, D. Nappo, F. Boccacci, S. Fattorini, and J. San-Miguel-Ayanz, *Nature Communications* **5**, 4114 (2014).
- [25] C. J. Carstens, *Physical Review E* **91**, 1 (2015).
- [26] A. R. Benson, *SIAM Journal on Mathematics of Data Science* **1**, 293 (2019).
- [27] G. F. de Arruda, G. Petri, P. M. Rodriguez, and Y. Moreno, *arXiv preprint arXiv:2112.04273* (2021).
- [28] I. Iacopini, G. Petri, A. Baronchelli, and A. Barrat, *Communications Physics* **5**, 64 (2022).
- [29] G. St-Onge, I. Iacopini, V. Latora, A. Barrat, G. Petri, A. Allard, and L. Hébert-Dufresne, *Communications Physics* **5**, 25 (2022).

APPENDIX A. APPROXIMATING THE HYPERGRAPH CONFIGURATION MODEL (HCM).

The ‘sparse-case’ approximation of the HCM allows us to greatly simplify the calculations in case $\rho = T/NL \ll 1$ (i.e. the density of 1s is much less than 1). In order to derive it, let us consider that the generic probability coefficient induced by the HCM can be Taylor-expanded as follows

$$p_{i\alpha} = \frac{x_i y_\alpha}{1 + x_i y_\alpha} = x_i y_\alpha - (x_i y_\alpha)^2 + (x_i y_\alpha)^3 \dots \quad (14)$$

and one may wonder the order at which the expansion can be truncated. It turns out that just considering the first order is enough to obtain predictions as accurate as those achievable under the ‘full’ HCM: in other words, one can simply put $p_{i\alpha}^{\text{FOA}} \simeq x_i y_\alpha$. Upon doing so, the system of equations defining the HCM simplifies to

$$k_i^* = \sum_{\alpha=1}^L x_i y_\alpha, \quad \forall i \quad (15)$$

$$h_\alpha^* = \sum_{i=1}^N x_i y_\alpha, \quad \forall \alpha \quad (16)$$

expressions leading us to find $x_i = k_i^*/\sqrt{T^*}$, $\forall i$ and $y_\alpha = h_\alpha^*/\sqrt{T^*}$, $\forall \alpha$. As a consequence, $p_{i\alpha}^{\text{FOA}} = x_i y_\alpha = k_i^* h_\alpha^*/T^*$ - a position that is commonly named Chung-Lu approximation (CLA). Figure 3 shows the goodness of the latter one in approximating $\langle \sigma_i \rangle_{\text{HCM}}$ for the **contact-primary-school**, the **email-Enron** and the **congress-bills** data sets, i.e. the accuracy of the following chain of equalities

$$\langle \sigma_i \rangle_{\text{HCM}} = \sum_{\alpha=1}^L p_{i\alpha}^{\text{HCM}} (h_\alpha - p_{i\alpha}^{\text{HCM}}) \stackrel{\text{FOA}}{\simeq} \sum_{\alpha=1}^L x_i y_\alpha (h_\alpha - x_i y_\alpha) \stackrel{\text{CLA}}{\simeq} \frac{k_i^*}{T^*} \left(1 - \frac{k_i^*}{T^*} \right) \sum_{\alpha=1}^L (h_\alpha^*)^2. \quad (17)$$

APPENDIX B. PARTIAL CONFIGURATION MODELS FOR BINARY, UNDIRECTED HYPERGRAPHS.

As we said in the main text, the HCM reduces to a ‘partial’ Configuration Model in case one of two degree sequences is left unconstrained.

Partial Configuration Model-I. For instance, let us constrain only the degree sequence $\{k_i\}_{i=1}^N$, $\forall i$, putting $\beta_\alpha = 0$, $\forall \alpha$ (or, equivalently, $y_\alpha = 1$, $\forall \alpha$). Our canonical probability distribution becomes

$$P(\mathbf{I}) = \prod_{i=1}^N \prod_{\alpha=1}^L \frac{x_i^{I_{i\alpha}}}{1 + x_i} = \prod_{i=1}^N p_i^{k_i} (1 - p_i)^{L - k_i} \quad (18)$$

where $e^{-\alpha_i} \equiv x_i$ and $p_i \equiv x_i/(1 + x_i)$, $\forall i$. The entries of the incidence matrix are, now, independent random variables obeying the Bernoulli probability mass functions

$$I_{i\alpha} \sim \text{Ber}(p_i), \quad \forall i, \alpha. \quad (19)$$

While the entries along the same column obey different distributions, the ones lying along the same row, instead, obey the same distribution. As a consequence, the i -th node degree, defined as a sum of i.i.d. Bernoulli random variables, obeys the binomial distribution

$$k_i \sim \text{Bin}(L, p_i), \quad \forall i; \quad (20)$$

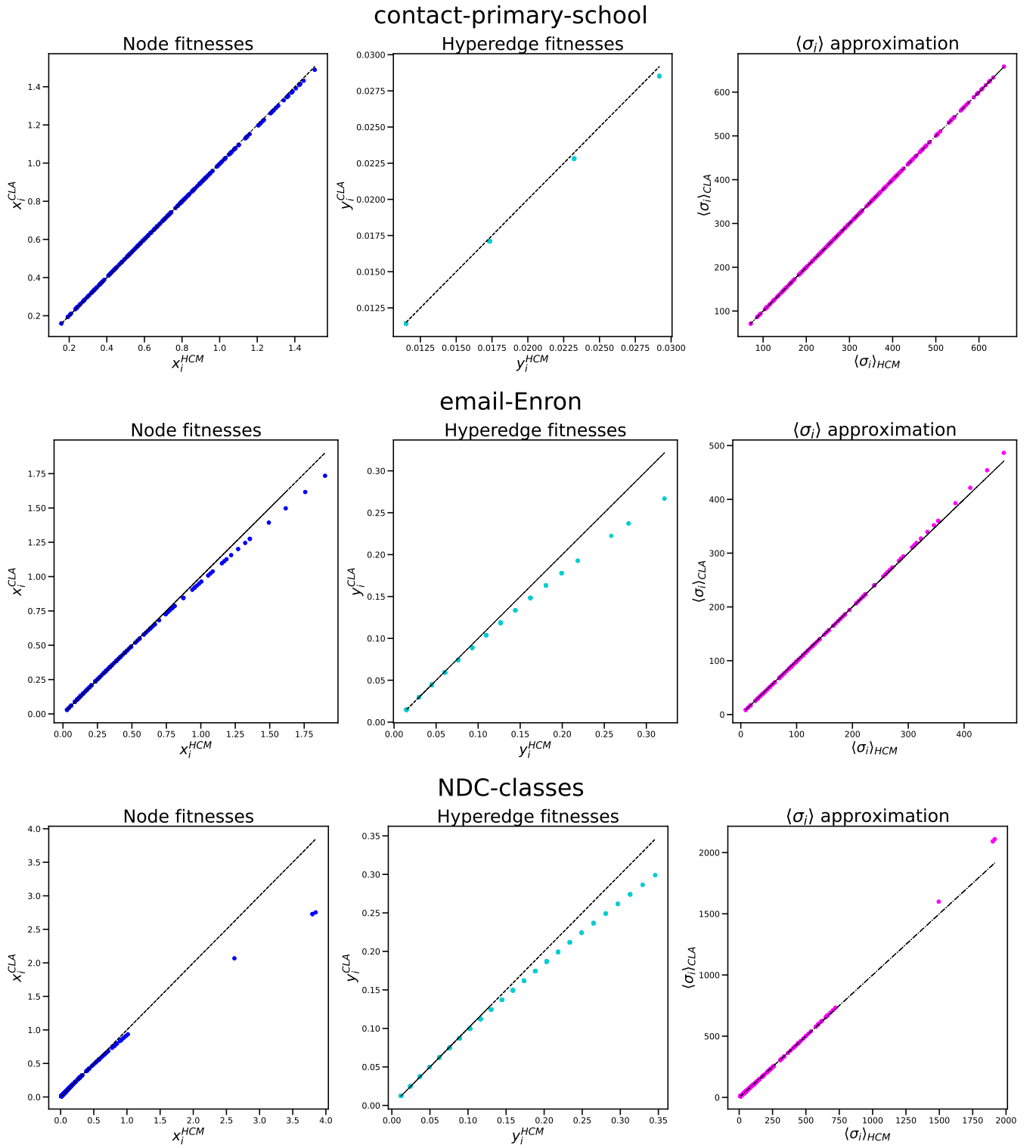


FIG. 3: Left panels: scatter plots between the numerical values of the node-specific Lagrange multipliers obtained by solving the ‘full’ HCM and the ones derived by adopting the CLA. Middle panels: scatter plots between the numerical values of the hyperedge-specific Lagrange multipliers obtained by solving the ‘full’ HCM and the ones derived by adopting the CLA. Right panels: scatter plots between the expected values $\{\langle \sigma_i \rangle_{HCM}\}$ and $\{\langle \sigma_i \rangle_{CLA}\}$.

the α -th hyperedge degree, instead, is defined as a sum of independent, but not equally distributed, Bernoulli random

variables: hence it obeys the Poisson-Binomial distribution

$$h_\alpha \sim \text{PB}(N, p_1 \dots p_N), \forall \alpha. \quad (21)$$

Quite interestingly, while the degrees of nodes obey different Binomial distributions, the degrees of hyperedges obey the same Poisson-Binomial distribution.

The resolution of the likelihood maximisation problem leads one to find the values $p_i = k_i^*/L$, $\forall i$ which, in turn, ensure that $\langle k_i \rangle_{\text{PCM-I}} = \sum_{\alpha=1}^L p_i = k_i^*$, $\forall i$ and that $\langle T \rangle_{\text{PCM-I}} = T^*$; instead, $\langle h_\alpha \rangle_{\text{PCM-I}}$ will, in general, be different from h_α^* - in fact, $\langle h_\alpha \rangle_{\text{PCM-I}} = T^*/L$, $\forall \alpha$.

From a microcanonical perspective, the number of configurations on which the degrees of nodes match their empirical values amounts at

$$\Omega_{\text{PCM-I}} = \prod_{i=1}^N \binom{L}{k_i^*}; \quad (22)$$

reshuffling the 1s along each row of the incidence matrix separately ensures the degrees of nodes to be preserved, while destroying any other correlation.

Partial Configuration Model-II. Analogously, the canonical probability distribution describing the case in which only the hyperedge degree sequence $\{h_\alpha\}_{\alpha=1}^L$ is constrained reads

$$P(\mathbf{I}) = \prod_{i=1}^N \prod_{\alpha=1}^L \frac{y_\alpha^{I_{i\alpha}}}{1 + y_\alpha} = \prod_{\alpha=1}^L p_\alpha^{h_\alpha} (1 - p_\alpha)^{N - h_\alpha} \quad (23)$$

where $e^{-\beta_\alpha} \equiv y_\alpha$ and $p_\alpha \equiv y_\alpha / (1 + y_\alpha)$, $\forall i, \alpha$. As for the previous null model, the entries of the incidence matrix are independent random variables obeying different Bernoulli probability mass functions, i.e.

$$I_{i\alpha} \sim \text{Ber}(p_\alpha), \forall i, \alpha; \quad (24)$$

the i -th node degree is defined as a sum of independent, but not equally distributed, Bernoulli random variables, hence it obeys the Poisson-Binomial distribution

$$k_i \sim \text{PoisBin}(L, p_1 \dots p_L), \forall i. \quad (25)$$

On the other hand, the α -th hyperedge degree is defined as a sum of i.i.d. Bernoulli random variables, hence it obeys the binomial distribution

$$h_\alpha \sim \text{Bin}(N, p_\alpha), \forall \alpha; \quad (26)$$

while the degrees of nodes obey the same Poisson-Binomial distribution, the degrees of hyperedges obey different binomial distributions.

The resolution of the likelihood maximisation problem leads one to find the values $p_\alpha = h_\alpha^*/N$, $\forall \alpha$ which, in turn, ensure that $\langle h_\alpha \rangle_{\text{PCM-II}} = \sum_{i=1}^N p_\alpha = h_\alpha^*$, $\forall \alpha$ and that $\langle T \rangle_{\text{PCM-II}} = T^*$; instead, $\langle k_i \rangle_{\text{PCM-II}}$ will, in general, be different from k_i^* - in fact, $\langle k_i \rangle_{\text{PCM-II}} = \sum_{\alpha=1}^L p_\alpha = T^*/N$, $\forall i$.

From a microcanonical perspective, the number of configurations on which the degrees of hyperedges match their empirical values amounts at

$$\Omega_{\text{PCM-II}} = \prod_{\alpha=1}^L \binom{N}{h_{\alpha}^*}; \quad (27)$$

reshuffling the 1s along each column of the incidence matrix separately ensures the degrees of hyperedges to be preserved, while destroying any other correlation.

	Total number of 1s, $\langle T \rangle$	Degrees of nodes, $\langle k_i \rangle$	Degrees of hyperedges, $\langle h_{\alpha} \rangle$
<i>Random Hypergraph Model</i>	T^*	T^*/N	T^*/L
<i>Partial Configuration Model-I</i>	T^*	k_i^*	T^*/L
<i>Partial Configuration Model-II</i>	T^*	T^*/N	h_{α}^*
<i>Hypergraph Configuration Model</i>	T^*	k_i^*	h_{α}^*

TABLE II: Summary of the constraints defining the canonical version of each model for randomising binary, undirected hypergraphs considered here. While the total number of 1s is preserved by each model, the degrees are separately preserved by the two partial versions of the HCM and jointly preserved by the HCM only. Stars indicate the empirical values of the constraints.

APPENDIX C. CALCULATING THE EXPECTED VALUE OF TOPOLOGICAL QUANTITIES.

Let us now provide the explicit expression of the expected value of some topological properties of interest. Let us start with the entries of the matrix \mathbf{W} , for which the following results hold true

$$\langle w_{ij} \rangle = \sum_{\alpha=1}^L \langle I_{i\alpha} I_{j\alpha} \rangle = \sum_{\alpha=1}^L \langle I_{i\alpha} \rangle \langle I_{j\alpha} \rangle = \sum_{\alpha=1}^L p_{i\alpha} p_{j\alpha}, \quad (28)$$

$$\text{Var}[w_{ij}] = \sum_{\alpha=1}^L \text{Var}[I_{i\alpha} I_{j\alpha}] + 2 \sum_{\beta < \gamma} \text{Cov}[I_{i\beta} I_{j\beta}, I_{i\gamma} I_{j\gamma}] = \sum_{\alpha=1}^L p_{i\alpha} p_{j\alpha} (1 - p_{i\alpha} p_{j\alpha}). \quad (29)$$

Therefore,

$$\sum_{\substack{j=1 \\ (j \neq i)}}^N \langle w_{ij} \rangle^2 = \sum_{\alpha=1}^L p_{i\alpha}^2 \left[\sum_{j=1}^N p_{j\alpha}^2 - p_{i\alpha}^2 \right] + 2 \sum_{\beta < \gamma} p_{i\beta} p_{i\gamma} \left[\sum_{j=1}^N p_{j\beta} p_{j\gamma} - p_{i\beta} p_{i\gamma} \right], \quad (30)$$

$$\sum_{\substack{j=1 \\ (j \neq i)}}^N \text{Var}[w_{ij}] = \sum_{\alpha=1}^L p_{i\alpha} (\langle h_{\alpha} \rangle - p_{i\alpha}) - \sum_{\alpha=1}^L p_{i\alpha}^2 \left[\sum_{j=1}^N p_{j\alpha}^2 - p_{i\alpha}^2 \right]. \quad (31)$$

Let us now consider the strength sequence of matrix \mathbf{W} , for which the following results hold true

$$\langle \sigma_i \rangle = \sum_{\alpha=1}^L p_{i\alpha} (\langle h_{\alpha} \rangle - p_{i\alpha}), \quad (32)$$

$$\text{Var}[\sigma_i] = \sum_{\substack{j=1 \\ (j \neq i)}}^N \text{Var}[w_{ij}] + 2 \sum_{\substack{j < k \\ (j, k \neq i)}} \text{Cov}[w_{ij}, w_{ik}] = \sum_{\substack{j=1 \\ (j \neq i)}}^N \text{Var}[w_{ij}] + 2 \sum_{\substack{j < k \\ (j, k \neq i)}} [\langle w_{ij} w_{ik} \rangle - \langle w_{ij} \rangle \langle w_{ik} \rangle]. \quad (33)$$

As a consequence, the expected value of the disparity ratio reads

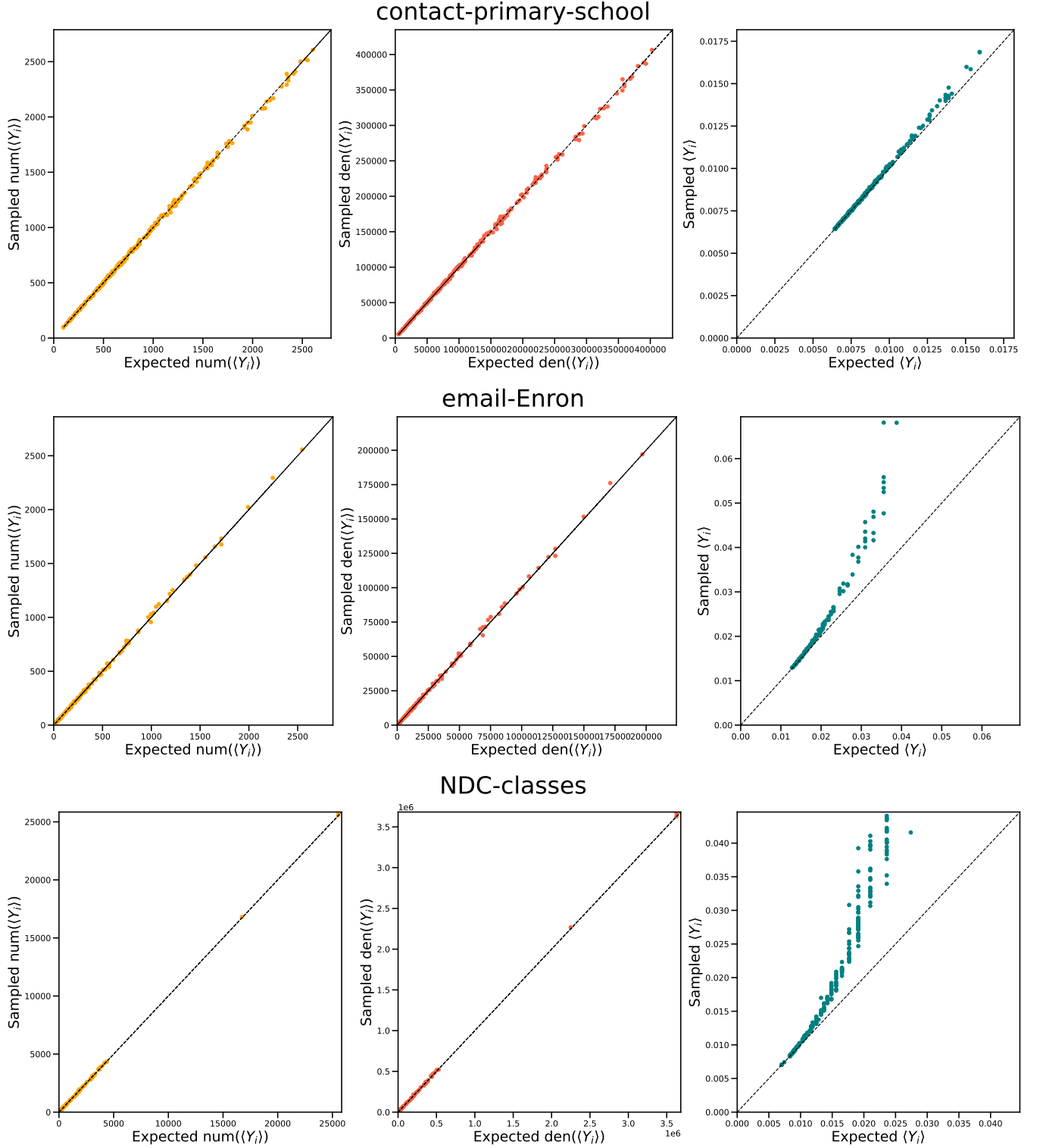


FIG. 4: Left panels: scatter plots between the numerical values of the numerator of the disparity ratio obtained analytically, by implementing the ‘full’ HCM and the ones derived by explicitly sampling the ensemble induced by it. Middle panels: scatter plots between the numerical values of the denominator of the disparity ratio obtained analytically, by implementing the ‘full’ HCM and the ones derived by explicitly sampling the ensemble induced by it. Right panels: scatter plots between the expected values $\{\langle Y_i \rangle_{\text{HCM}}\}$ computed as in Eq.(34) and the ones obtained by explicitly sampling the ensemble induced by the ‘full’ HCM. As approximated and sampled values of both numerators and denominators nicely agree, the result concerning $\{\langle Y_i \rangle\}$ must be imputed to the correlation between the two which is disregarded by Eq.(34).

$$\langle Y_i \rangle \simeq \sum_{\substack{j=1 \\ (j \neq i)}}^N \frac{\langle w_{ij}^2 \rangle}{\langle \sigma_i^2 \rangle} = \sum_{\substack{j=1 \\ (j \neq i)}}^N \frac{\langle w_{ij} \rangle^2 + \text{Var}[w_{ij}]}{\langle \sigma_i \rangle^2 + \text{Var}[\sigma_i]} \quad (34)$$

where the \simeq symbol is understood to approximate the expected value of a ratio as the ratio of expected values. This approximation just represents the first order of the Taylor expansion

$$\mathbb{E} \left[\frac{X}{Y} \right] \simeq \frac{\mathbb{E}[X]}{\mathbb{E}[Y]} - \frac{\text{Cov}[X, Y]}{\mathbb{E}[Y]^2} + \frac{\mathbb{E}[X]}{\mathbb{E}[Y]^3} \text{Var}[X]; \quad (35)$$

due to the correlation between numerator and denominator, the second and the third terms of Eq.(35) may not be negligible: as Fig. 4 shows, while Eq.(34) holds true for the **contact-primary-school** data set, it does not for the other two ones.

APPENDIX D. CALCULATING THE EXPECTED VALUE OF THE CONFUSION MATRIX ENTRIES.

Before defining the entries of the confusion matrix, let us call $\tilde{\mathbf{I}}$ the generic incidence matrix in the ensemble induced by one of the models considered in the present paper. The expected value of any quantity which is a function of $\tilde{\mathbf{I}}$ is readily calculated by averaging it over the ensemble of incidence matrices induced by the same model.

The positive rate (TPR) is defined as the percentage of links correctly recovered by a given method and reads

$$TPR = \frac{TP}{T} = \frac{\sum_{i < j} I_{i\alpha} \tilde{I}_{i\alpha}}{T} \implies \langle TPR \rangle = \frac{\langle TP \rangle}{T} = \frac{\sum_{i < j} I_{i\alpha} p_{i\alpha}}{T}; \quad (36)$$

the specificity (SPC) is defined as the percentage of 0s correctly recovered by a given method and reads

$$SPC = \frac{TN}{NL - T} = \frac{\sum_{i < j} (1 - I_{i\alpha})(1 - \tilde{I}_{i\alpha})}{NL - T} \implies \langle SPC \rangle = \frac{\langle TN \rangle}{NL - T} = \frac{\sum_{i < j} (1 - I_{i\alpha})(1 - p_{i\alpha})}{NL - T} \quad (37)$$

the positive predictive value (PPV) is defined as the percentage of links correctly recovered by a given method with respect to the total number of predicted links and reads

$$PPV = \frac{\sum_{i < j} I_{i\alpha} \tilde{I}_{i\alpha}}{\tilde{T}} \implies \langle PPV \rangle = \frac{\langle TP \rangle}{\langle T \rangle} = \frac{\sum_{i < j} I_{i\alpha} p_{i\alpha}}{\langle T \rangle}; \quad (38)$$

lastly, the accuracy (ACC) measures the overall performance of a given reconstruction method in correctly placing both links and 0s and reads

$$ACC = \frac{TP + TN}{NL} \implies \langle ACC \rangle = \frac{\langle TP \rangle + \langle TN \rangle}{NL}. \quad (39)$$

As stressed in the main text, results on the confusion matrix of a number of real-world hypergraphs reveal that the large sparsity of the latter ones makes it difficult to reproduce the TPR and the PPV (see Table III); on the other hand, the capability of the HCM to reproduce the density of 1s of an incidence matrix makes it capable of recovering the density of 0s as well, thus ensuring the overall accuracy of the model to be quite large.

Data set	$\langle TPR \rangle$	$\langle SPC \rangle$	$\langle PPV \rangle$	$\langle ACC \rangle$	ρ
coauth-DBLP	1.95×10^{-5}	1.000	1.95×10^{-5}	1.000	1.63×10^{-6}
coauth-MAG-History	1.04×10^{-5}	1.000	1.04×10^{-5}	1.000	1.51×10^{-6}
coauth-MAG-Geology	3.30×10^{-5}	1.000	3.30×10^{-5}	1.000	2.51×10^{-6}
congress-bills	0.018	0.995	0.018	0.99	5.04×10^{-3}
contact-high-school	0.009	0.993	0.009	0.986	7.12×10^{-3}
contact-primary-school	0.013	0.990	0.013	0.980	1.00×10^{-2}
DAWN	0.043	0.999	0.043	0.997	1.54×10^{-3}
email-Enron	0.048	0.980	0.048	0.960	2.10×10^{-2}
email-Eu	0.016	0.997	0.016	0.993	3.43×10^{-3}
NDC-classes	0.089	0.995	0.089	0.991	5.10×10^{-3}
NDC-substances	0.030	0.999	0.030	0.998	1.02×10^{-3}
tags-ask-ubuntu	0.018	0.999	0.018	0.998	1.12×10^{-3}
tags-math-sx	0.022	0.998	0.022	0.996	2.14×10^{-3}
threads-ask-ubuntu	0.001	1.000	0.001	1.000	1.52×10^{-5}
threads-math-sx	0.002	1.000	0.002	1.000	1.39×10^{-5}

TABLE III: Confusion matrix and density of 1s for a number of real-world hypergraphs.

APPENDIX E. CALCULATING THE CLIQUE MOTIF EIGENVECTOR CENTRALITY.

The clique motif eigenvector centrality (CEC) has been proposed in [26]: its i -th entry, CEC_i , is nothing else than the corresponding entry of the Perron-Frobenius eigenvector of \mathbf{W} .

In order to evaluate the expected value of the CEC we have explicitly sampled the ensemble of incidence matrices induced by the HCM; then, we have calculated the matrix $\tilde{\mathbf{W}}$ induced by each $\tilde{\mathbf{I}}$ according to Eq.(8). Afterwards, we have calculated the Perron-Frobenius eigenvector of each ‘projected’ matrix and taken their average in an entry-wise fashion.

Remarkably, we found that the aforementioned ensemble average basically coincides with the Perron-Frobenius eigenvector of the ensemble average of \mathbf{W} itself, i.e. $\langle \mathbf{W} \rangle_{\text{HCM}}$, as Fig. 5 shows.

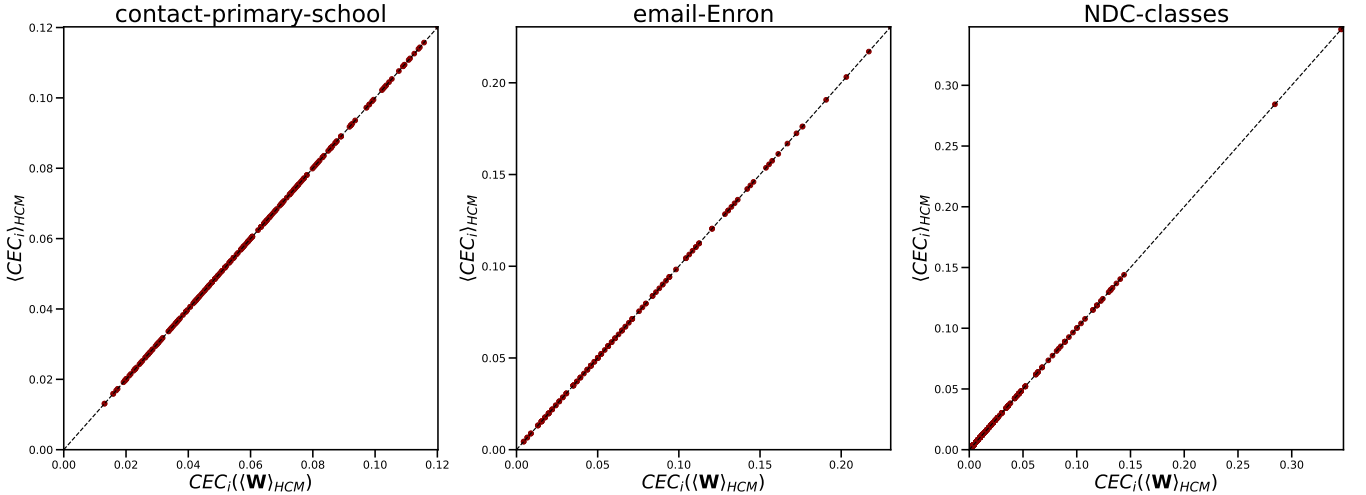


FIG. 5: Scatter plot between the numerical values of each component of the CEC, calculated by taking the ensemble average of the Perron-Frobenius eigenvector of each matrix $\tilde{\mathbf{W}}$, induced by $\tilde{\mathbf{I}}$ according to Eq.(8), and the corresponding component of the Perron-Frobenius eigenvector of $\langle \mathbf{W} \rangle_{\text{HCM}}$. The extremely good agreement suggests a faster way of calculating the CEC that avoids to explicitly sample the ensemble induced by a particular null model.

APPENDIX F. COMPARISON BETWEEN THE RHM AND THE HCM ACCURACY.

Let us now inspect the accuracy of the RHM and of the HCM in reproducing patterns of real-world hypergraphs. To this aim, let us consider the quantity also known as coefficient of determination and defined as

$$R^2 = 1 - \frac{SS_{\text{res}}}{SS_{\text{tot}}}; \quad (40)$$

in our case, it can be re-defined as

$$R^2_{\text{null-model}}(X) = 1 - \frac{\sum_i (X_i - \langle X_i \rangle_{\text{null-model}})^2}{\sum_i (X_i - \bar{X})^2} \quad (41)$$

and interpreted as measuring the goodness of a null model to reproduce empirical data when compared to a baseline model whose only prediction reads \bar{X} , i.e. the arithmetic mean of the empirical data themselves. Such a model achieves an R^2 which is 0 while a model that is capable of matching the observed values exactly achieves an R^2 which is 1; models that achieve worse predictions than the baseline model (i.e. their discrepancies are larger) have a negative R^2 .

As Table IV shows, the HCM is, overall, more accurate than the RHM in reproducing the quantities we have considered (i.e. the sigma and the CEC). While few cases are met for which the HCM performs worse than the baseline model, the RHM, on the other hand, is found to steadily perform worse than it when the CEC is considered and to perform quite similar to it when the sigma is considered. Overall, these results confirm that just constraining the total number of 1s of an incidence matrix is not enough to achieve an accurate description of the corresponding, real-world hypergraph.

Data set	$R^2_{\text{HCM}}(\sigma)$	$R^2_{\text{HCM}}(\text{CEC})$	$R^2_{\text{RHG}}(\sigma)$	$R^2_{\text{RHG}}(\text{CEC})$
coauth-DBLP	0.840	-0.886	$\simeq 0$	-0.987
coauth-MAG-History	0.459	-0.504	-0.002	-0.989
coauth-MAG-Geology	0.875	-0.693	-0.002	-0.962
congress-bills	0.917	0.718	-0.101	-0.293
contact-high-school	-0.716	0.393	-1.124	0.011
contact-primary-school	-1.186	0.798	-1.418	0.329
DAWN	0.914	0.949	$\simeq 0$	-0.670
email-Enron	0.765	0.607	-0.009	-0.094
email-Eu	0.775	0.038	-0.044	-0.492
NDC-classes	0.821	0.775	-0.008	-0.592
NDC-substances	0.963	0.865	-0.016	-0.572
tags-ask-ubuntu	0.895	0.914	-0.004	-0.594
tags-math-sx	0.893	0.850	-0.008	-0.547
threads-ask-ubuntu	0.807	0.443	-0.003	-0.836
threads-math-sx	0.859	0.911	-0.001	-0.819

TABLE IV: The R^2 index allows us to inspect and compare the accuracy of the RHM and of the HCM in reproducing patterns of real-world hypergraphs. The HCM is, overall, more accurate than the RHM in reproducing the quantities we have considered. While the HCM still performs worse than the baseline model in a few cases, the RHM, on the other hand, is found to steadily perform worse than it when the CEC is considered and to perform quite similar to it when the sigma is considered. Overall, just constraining the total number of 1s of an incidence matrix is not enough to achieve an accurate description of the corresponding, real-world hypergraph.